Synthesis and Spectral Characterization Studies of New Trimethoprim-Diphenylphosphate Metal Complexes

Abdel-Nasser M. A. Alaghaz[1], Rabie S. Farag[2], Mohammed A. Elnawawy[3], Ahmed D. A. Ekawy[4]

[1, 2, 3, 4]Department of Chemistry, Faculty of Science, Al–Azhar University, Nasr City, Cairo, Egypt. (E mail address:

Abstract: *Eight mononuclear Mn(II), Fe(III), Co(II), Ni(II), Cu(II), Zn(II), Pb(II) and La(III) complexes of DPTMEBPP ligand were synthesized and determined by different physical techniques. The molar ratio for all synthesized complexes is M: DPTMEBPP = 1:1 which was established from the results of chemical analysis. All the eight metal complexes are reported using elemental analysis, molar conductance, magnetic susceptibility, IR, UV–Vis, thermal analysis and ^{1}H-NMR, ^{13}C NMR, mass, XRD spectral studies. The molar conductance measurements of all the complexes in DMSO solution correspond to nonelectrolytic nature. The crystal field splitting, Racah repulsion and nepheloauxetic parameters and determined from the electronic spectra of the complexes. The presence of co-ordinated water molecules were confirmed by thermal studies. All complexes were of the high-spin type and found to have six-coordinate octahedral geometry except the Cu(II), Zn(II) and Pb(II) complexes which were four coordinate, square planar geometry for Cu(II) complex while tetrahedral geometry for Zn(II) and Pb(II) complexes.*

Keywords: Trimethoprim; diphenylphosphate; Transition metal complexes; Spectra

1. Introduction

Trimethoprim, chemically 5-(3,4,5-trimethoxybenzyl) pyrimidine-2,4-diamine, belongs to the class of chemotherapeutic agents known as dihydrofolate reductase inhibitors. It is used in prophylaxis treatment and urinary tract infections [1]. The application of inorganic chemistry to medicine ("Elemental Medicine") is a rapidly developing field, and novel therapeutic and diagnostic metal complexes have an impact on medical practice. Advances in biocoordination chemistry are crucial for improving the design of compounds to reduce toxic side-effects and understand their mechanisms of action. Most of the major classes of pharmaceutical agents contain examples of metal compounds which are in current clinical use [2], and new areas of application are rapidly emerging. Some of these are discussed briefly below with special emphasis on the targeting of metal complexes and their bio-transformation. Targeting is important because the toxicity is often associated with metal compounds. If they can be delivered only to the tissues, cells and receptors where they are required, the toxicity may be reduced. The ease with which many metal complexes undergo ligand substitution and redox reactions is likely to mean that the active species are bio-transformation products of the administered complex. Identification of these active species will lead to the more effective use of metal compounds as drugs. Compounds containing pyrimidine rings play a significant role in many biological systems [3]. The pyrimidine ring system, present in nucleic acids, several vitamins, coenzymes and antibiotics, provides potential binding sites for metal ions, and any information on their coordinating properties is important as a means of understanding the role of the metal ions in biological systems. Many compounds of therapeutic importance contain the pyrimidine ring system. So, substituted 2,4-diaminopyrimidines are widely employed as metabolic inhibitors of pathways leading to the synthesis of proteins and nucleic acids. Among these kinds of ligands, TMP is a well known biological agent, also employed as a potent metabolic inhibitor of bacterial dihydrofolic acid reductase. Trimethoprim has potential binding sites for metal ions. Several authors have studied the interaction of this ligand with biological metal ions and the coordination of TMP via a NH_2 nitrogen atom has been inferred on the basis of IR and visible measurements [4,5]. However, other authors have shown by X-ray diffraction methods that the coordination site of the TMP molecule is the N1 of the pyrimidine ring [6–10]. On the other hand, more recently, other research groups [11–16] have prepared and characterized complexes of TMP with metal(II)/(III) and the spectral and analytical data show that the ligand acts as a monodentate or bidentate.

The present work is focused on preparation and structural elucidation of a new ligand, diphenyl (2-amino-5-(3,4,5-trimethoxybenzyl)pyrimidin-4-yl-phosphoramidate (DPTMEBPP) as well as its complexes with Mn(II), Fe(III), Co(II), Ni(II), Cu(II), Zn(II), Pb(II) and La(III) metal ions.

2. Experimental

2.1. Synthesis of diphenyl (2-amino-5-(3,4,5-trimethoxybenzyl)pyrimidin-4-yl-phosphoramidate (DPTMEBPP)

Asolution of diphenylcholrophosphate (6.2 ml, 0.03 mole) indry benzene(100ml)was added dropwise toawell stirred solution of trimethoprim ([17] 8.7 gm, 0.03 mole) and triethyl amin (4.16 ml , 0.03 mole) in drybenzene after the complete addition of diphenylchlorophosphate on cooling. The mixture was heated under reflux for 5 hours. The formed solid (triethylaminehydrochlorid) was filtered off and filterate was evaporated under vacuo obtain solid was recrystallized from ethanol give (13.5 gm, 85% yield) white bowder m.p (158-160) under reflux for three hours. The purity of the product was checked was by TLC. Yield: 92% and the melting point is 132 ºC (Table 1).

Paper ID: NOV152999

2.2. Synthesis of metal (II/III) complexes

Solution of manganese acetate $Mn(CH_3COO)_2.4H_2O$, Iron nitrate $Fe(NO_3)_3.9H_2O$, cobalt acetate $Co(CH_3COO)_2.4H_2O$, nickle $Ni(CH_3COO)_2.4H_2O$, copper acetate $Cu(CH_3COO)_2.H_2O$, zinc acetate $Zn(CH_3COO)_2.2H_2O$, Lead acetate $pb(CH_3COO)_2. 2H_2O$ and Lanthanium cholorid $LaCl_3.7H_2O$ (0.002 mole) in dry ethanol (50ml) were added dropwies to a solution of [(I) 0.002 mole] at room temperature with continuous stirring, the reaction mixture was heated data are listed in Table 1.

Table 1: Elemental analysis and Physico-analytical data for DPTMEBPP ligand and its metal complexes

Cpd. M. F. [M.Wt]	m.p. (°C)	Color [Yield (%)]	Elemental analyses % calculated (found)						$^a\Lambda_m$
			M	C	H	N	P	Cl	
[DPTMEBPP] $C_{26}H_{27}N_4O_6P$ [522.49]	132	Brown[88]	–	59.77 (59.65)	5.21 (5.14)	10.72 (10.63)	5.93 (5.87)	–	–
(1)[Mn(DPTMEBPP)(H$_2$O)$_2$(OAc)$_2$]2H$_2$O $C_{30}H_{41}MnN_4O_{14}P$ [767.58]	189	Apple-green [89]	7.16 (7.16(	46.94 (46.94)	5.38 (5.38)	7.30 (7.30)	4.04 (4.04)	–	20.20
(2)[Fe(DPTMEBPP)(H$_2$O)(NO$_3$)$_3$]6.75H$_2$O $C_{26}H_{42.5}FeN_7O_{22.75}P$ [903.97]	192	Orange-red [90]	6.18 (6.18(	34.55 (34.55)	4.74 (4.74)	10.85 (10.85)	3.43 (3.43)	–	17.33
(3)[Co(DPTMEBPP)(H$_2$O)$_2$(OAc)$_2$]2H$_2$O $C_{30}H_{41}CoN_4O_{14}P$[771.57]	188	Cannery-yellow [88]	7.64 (7.64(	46.70 (46.70)	5.36 (5.36)	7.26 (7.26)	4.01 (4.01)	–	18.05
(4)[Ni(DPTMEBPP)(H$_2$O)$_2$(OAc)$_2$]2H$_2$O $C_{30}H_{41}N_4NiO_{14}P$ [771.33]	186	Green [91]	7.61 (7.61(	46.71 (46.63)	5.36 (5.36)	7.26 (7.32)	4.02 (4.02(	–	16.53
(5)[Cu(DPTMEBPP)(OAc)$_2$]H$_2$O $C_{30}H_{35}CuN_4O_{11}P$ [722.14]	193	Dark green [90]	8.80 (8.80(	49.90 (49.90)	4.89 (4.89)	7.76 (7.34)	4.29 (4.29)	–	15.55
(6)[Zn(DPTMEBPP)(OAc)$_2$]2H$_2$O $C_{30}H_{37}N_4O_{12}PZn$ [741.99]	197	Dark brown [84]	8.81 (8.68(	48.56 (48.35)	5.03 (4.97)	7.55 (7.33)	4.17 (4.12)	–	10.12
(7)[Pb(DPTMEBPP)(OAc)$_2$]3H$_2$O $C_{30}H_{39}N_4O_{13}PPb$ [901.82]	187	Orange [88]	22.98 (22.83(	39.95 (39.95)	3.30 (3.29)	7.06 (7.00)	3.43 (3.34)	–	10.25
(8)[La(DPTMEBPP)(H$_2$O)Cl$_3$]6H$_2$O $C_{26}H_{41}Cl_3LaN_4O_{13}P$ [893.86]	187	Orange [88]	14.16 (14.14(	34.94 (34.38)	4.62 (4.52)	6.27 (6.15)	3.47 (3.40)	11.90 (11.73(	10.25

^{a} Λ_m: molar conductance $(\Omega^{-1} mo^{-1}cm^2)$

2.3. Physical Measurements

Elemental analyses (CHNS) were carried out on a Perkin Elmer CHNS 2400. The percentage of the metal ions were determined gravimetrically by transforming the solid products into metal oxide or sulfate and also determined by using atomic absorption method. The molar conductance of solid chelates in DMSO was measured using Sybron–Barnstead conductometer (Meter–PM.6, E = 3406). Their IR spectra were recorded on Perkin-Elmer FT–IR spectrophotometer in nujol mull and polyethylene pellets. The UV–visible absorption spectra were recorded using Jasco V–350 recording spectrophotometer at room temperature. Magnetic susceptibility of the metal complexes were measured by the Gouy method at room temperature using a Johnson Matthey, Alpha products, model MKI magnetic susceptibility balance and the effective magnetic moments were calculated using the relation μ_{eff} = 2.828 $(\chi_m \cdot T)^{1/2}$B·M, where χ_m is the molar susceptibility corrected using Pascal"s constants for diamagnetism of all atoms in the compounds. The mass spectra were recorded by the EI technique at 70 eV using MS-5988 GC–MS Hewlett–Packard instrument in the Microanalytical Center, Cairo University. The ^{1}H (300 MHz) and ^{13}C NMR (75 MHz) spectra were recorded using 300 MHz Varian–Oxford Mercury. The deuterated solvent used was dimethylsulphoxide (DMSO) and the spectra extended from 0 to 15 ppm. The TGA were recorded on a Shimadzu TGA–50 H. TGA was carried out in a dynamic nitrogen atmosphere (20mL min^{-1}) with a heating rate of 10 ºCmin^{-1}. EPR spectrum of Cu(II) the complex was recorded as polycrystalline samples, at room temperature, on an E4–EPR spectrometer using the DPPH as the *g*–marker. The X–ray diffraction patterns for the obtained CT complexes were collected on a PAN anlytical X'Pert PRO X–ray powder diffractometer at the Central Lab at college for girls, Ain Shams University, Egypt University, Egypt.

3. Results and Discussion

In this study, metal(II/III) complexes of DPTMEBPP have been prepared and characterized by the analytical and spectroscopic methods. The separated complexes are stable in air, insoluble in water and common organic solvents, but completely soluble in DMSO. The elemental analysis, color, and melting point together with the formula weight obtained from the mass spectra for the complexes are given in Table 1 and agree very well with molecular formula proposed. The analytical data show the composition of the metal complexes to be [Mn(DPTMEBPP)(OAc)$_2$(H$_2$O)$_2$].2H$_2$O, [Fe(DPTMEBPP)(NO$_3$)$_3$(H$_2$O)$_2$].6.75H$_2$O, [Co(DPTM-EBPP)(OAc)$_2$(H$_2$O)$_2$].2H$_2$O, [Ni(DPTMEBPP) (OAc)$_2$(H$_2$O)$_2$].2H$_2$O, [Cu(DPTMEBPP)-(OAc)$_2$].H$_2$O, [Zn(DPTMEBPP)(OAc)$_2$].2H$_2$O, [Pb(DPTMEBPP)-(OAc)$_2$].3H$_2$O and [La(DPTMEBPP)(Cl)$_3$(H$_2$O)$_2$].6H$_2$O. The ratios of the metal present in all complexes have been determined by atomic absorption spectroscopy. The complexes have been decomposed in HNO$_3$/HClO$_4$ (2/1) and then dissolved in 1.5 N HClO$_4$. The amounts of metals have been determined (Table 1). The molar conductivity measurements have been done all compounds in DMF ($\sim$1.10^{-3}M solutions). The conductivity data of the complexes are very low and they can be regarded as non–electrolytes[16]. Chloride ion in the [La(DPTMEBPP)(Cl)$_3$(H$_2$O)$_2$].6H$_2$O complex has been determined by titration with AgNO$_3$.

Various attempts, such as crystallization using mixtures of solvents and low temperatures, were unsuccessful for the growth of a single crystal suitable for X–ray crystallography. However, the analytical, spectroscopic and magnetic data enabled the possible structure of the synthesized complexes to be predicted. The DPTMEBPP ligand and its metal complexes which we studied have not been previously reported in the literature.

3.1 The DPTMEBPP ligand

The analytically pure ligand DPTMEBPP (Figure 1) was readily synthesized with very good yield (90%) by phosphoramidate reaction of TMP (5–(3,4,5–trimethoxybenzyl)-pyrimidine–2,4–diamine) with equimolar of diphenylchlorophosphate in acetonitrile. The ligand DPTMEBPP may show keto–enol tautomerism because it contains the phosphenous amide (–NH–P=O) bonds [18-21]. The IR spectrum does not show a ν(OH) band at or 3400 cm^{-1} but shows the band at 3273 cm^{-1} corresponding to ν(NH) [18-21], indicating that in solid state, the ligand exists in the keto form for the ligand DPTMEBPP. However, the ^{1}H NMR spectrum of ligand shows a singlet at 9.75 ppm corresponding to OH groups which suggest the existence of ligand in enolic form in solution. The ^{31}P NMR of the ligand records a signal at δ=14.45 ppm, which supports the phosphenous amide group [18-21]. In the ^{13}C NMR spectrum three peaks at 163.8 ppm, 158.8 ppm, 58.3 ppm and 32.5 ppm were observed, being assigned to C=N, C–OP, CH$_2$ and CH$_3$, respectively. The electronic spectrum of DPTMEBPP in ethanol showed absorption bands at 240–390 nm regions which is due to intraligand $\pi \rightarrow \pi^*$ and n $\rightarrow \pi^*$ transitions involving molecular orbital of the pyrimidine ring, a broad shoulder at approximately 432 nm were observed. The latter band is attributed to an n(oxygen) $\rightarrow \pi^*$ transition of the dipolar zwitter ionic structure or keto–amine tautomer of DPTMEBPP [18-21]. The electron impact mass spectrum (Figure 2) of the free ligand, confirms the proposed formula by showing a peak at 522 u corresponding to the ligand moiety [(C$_{26}$H$_{27}$N$_4$O$_6$P) atomic mass 522 u]. The series of peaks in the range, i.e. 60,71,86,10,125, 149, 157, 179, 185, 199, 213, 236, 243, 256, 279, 292, 296, 309, 326, 348, 358, 368, 386, 395, 417, 432, 443, 452, 470, 491 and 509 u, etc., may be assigned to various fragments and their intensity gives an idea of stability of fragments. The mass spectrum of the ligand (DPTMEBPP) shows the fragmentation pattern in Scheme 1.
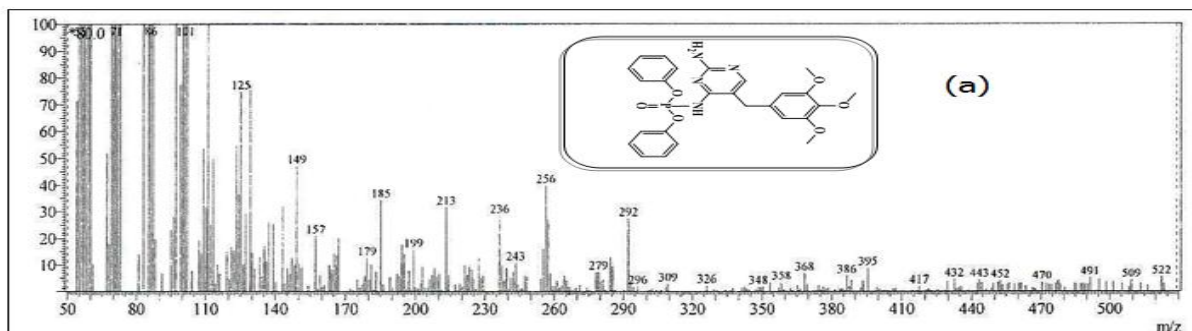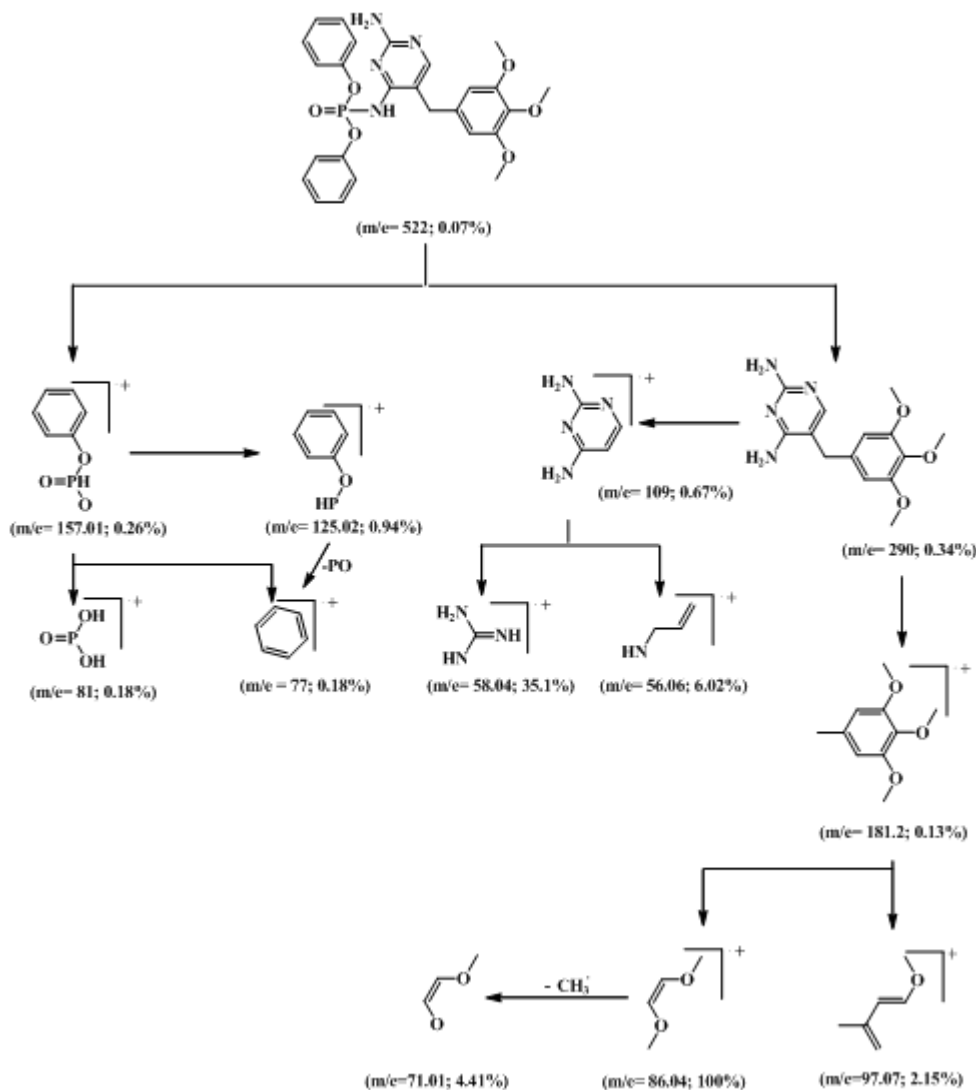
Figure 1: Proposed structure of DPTMEBPP ligand

Figure 2: Mass spectrum of DPTMEBPP ligand.

Scheme 1: Fragmentation pattern of DPTMEBPP ligand

3.2. Characterization of metal(II/III) complexes

3.2.1. Infrared spectra and mode of bonding

In the absence of a powerful technique such as X-ray crystallography, IR spectra have proven to be the most suitable technique to give enough information's to elucidate the nature of bonding of the ligand to the metal ion. The IR spectra of the free ligand and metal complexes were carried out in the range 4000–400 cm^{-1}. The IR spectra of the ligand and its metal complexes were found to be very similar to each other. DPTMEBPP possesses seven potential donor sites; two pyrimidinyl N atoms, one NH_2 and one NH groups on the pyrimidine rings, three methoxy groups and phosphate group. So, the ν_{as}(N–H) and ν_s(N–H) modes of the pyrimidine–NH_2 groups in the free DPTMEBPP are assigned to the strong and sharp bands at 3460 and 3312 cm^{-1}, respectively, which are affected by the presence of hydrogen bonds. In all the complexes the bands ν(N–H), due to asymmetric and symmetric vibrations, are present in the region 3480–3400 cm^{-1}; these bands shifted significantly with respect to those of the ligand. This confirms that the metal ion is coordinated to the trimethoprim through the two N atoms that belong to NH_2 and NH groups [1]. The (C=N) stretching vibration band of DPTMEBPP is observed at

1223

1650 cm^{-1}. Upon the complex formation, the (C=N) stretching vibration band is shifted to a lower wave number (between 1645 and 1600 cm^{-1}). In the IR spectra of the complexes, a bands are observed at 270– 294 and 320 – 328 cm^{-1} that is attributed to the ν(M–N) [22] and ν(M–Cl) [22] stretching vibrations, respectively. Another band appeared between 332 and 342 cm^{-1}, which is assigned to the interaction of phenolic oxygen to the metal atom, i.e., the stretching vibrations ν(M–O) [21]. Also, in the IR spectra of the complexes, a bands are observed at 187– 193 and 216– 233 cm^{-1} that is attributed to the ν(O–M–O) and ν(O–M–N) [23,24] stretching vibrations, respectively. The bands in the range 744–837 cm^{-1} and 614–633 cm^{-1} appeared in the spectra of these complexes which may be assigned to ρr(H$_2$O) and ρw(H$_2$O) [22]. IR spectra of nitrate complex displays three (N–O) stretching bands, at $\sim$1414 cm^{-1} (ν_5), 1305 cm^{-1} (ν_1) and 1004 cm^{-1} (ν_2). The separation of two highest frequency bands (ν_5–ν_1), Δ is 109 cm^{-1}. Suggesting that both the nitrate groups are coordinated to the central metal ion [24,25] in unidentate manner.

3.2.2. NMR spectra

The ^{1}H NMR spectra of the DPTMEBPP and its complexes have been recorded using DMSO. In the spectrum of the DPTMEBPP, the–CH$_2$ protons are seen at 3.42 ppm as singlet. The singlets in the 3.77 and 3.54 ppm can be attributed to the methoxy protons. The slightly broad bands at the 5.71 and 6.10 ppm can be attributed to the NH$_2$ and NH protons. The aromatic protons are shown at 6.58 and 7.55 ppm as singlets. In the spectra of the complexes, the NH$_2$ and NH protons have been shifted to the lower regions and this situation confirms that the nitrogen atom of the amine and imine groups coordinates to the metal ions. The signal observed at 3.33 ppm with an integration corresponding to four, four and fourteen protons in case of Zn(II), Pb(II) and La(III) complexes are assigned to two, three and eight water molecules, respectively.

3.2.3. Electronic spectra and magnetic behavior

The significant electronic spectra of the ligand and complexes are recorded in DMSO. The important bands of the ligand are observed in the region of 430–332 nm.

The magnetic moments of the complexes (as B.M.) were measured at room temperature. The effective magnetic moment values for Mn(DPTMEBPP), Fe(DPTMEBPP), Co(DPTMEBPP), Ni(DPTMEBPP) and Cu(DPTMEBPP) complexes were 5.98, 5.84, 5.08, 3.24 and 1.89 B.M., respectively. Low magnetic moment values support octahedral configurations for the Mn(II), Fe(III), Co(II), Ni(II) and Cu(II) complexes [23].

Electronic spectrum of the manganese(II) complex displays weak absorption bands at 18,178, 24,734, 29,633 and 31,835 cm^{-1} corresponding to an octahedral geometry. These bands may be assigned to ^{6}A$_1$g→^{4}T$_1$g (4G), ^{6}A$_1$g→^{4}E$_2$g, ^{4}A$_1$g (4G), ^{6}A$_1$g→^{4}E$_2$g (4D), and ^{6}A$_1$g→^{4}T$_1$g (4P) transitions, respectively [23]. Electronic spectrum of of the iron(III) complex exhibits three spectral bands at 16,542 (ν_1), 20,746 (ν_2) and 25,947cm^{-1} (ν_3) corresponding to an octahedral geometry [23]. Electronic spectrum of the cobalt(II) complex exhibits a broad band at 8827 cm^{-1} and two shoulders at 14,536 and 20,857 cm^{-1}. These bands may be assigned to ^{4}T$_1$g→^{4}T$_2$g (ν_1), ^{4}T$_1$g→^{4}A$_2$g (ν_2), and ^{4}T$_1$g→^{4}T$_2$g (P) (ν_3) transitions, respectively [24,25]. The low value of ν_2/ν_1 = 1.66 may be due to distortion of the octahedral structure. This is consistent with vary broad nature of the ν_1 band which may be assigned to the envelop of the transitions from ^{4}Eg (^{4}T$_1$g) to the components ^{4}B$_2$g and ^{4}Eg of ^{4}T$_2$g characteristic of tetragonally distorted octahedral environment. Electronic spectrum of the nickel(II) complex displays two well–defined bands at 10,664 and 16,623 cm^{-1}.These may be assigned to ^{3}A$_2$g→^{3}T$_2$g (F) (ν_1) and ^{3}A$_2$g→^{3}T$_1$g (F) (ν_2) transitions, respectively. In the present study splitting of ν_1 band was not observed which is generally observed in D$_4$h symmetry. So Dt, Dq^E, Dq^A cannot be calculated. The third d–d transitions band (ν_3) which may be obscured by the more intense charge transfer band was calculated to be at 24,614 cm^{-1}. All of these values, are characteristic of an octahedral geometry for the nickel(II) complex[24,25]. Electronic spectrum of the copper(II) complex displays bands at 10,169 (ε= 49Lmol^{-1} cm^{-1}), 18,586 (ε=64Lmol^{-1} cm^{-1}), and 30,336 cm^{-1} (ε = 85 L mol^{-1} cm^{-1}). First two bands may be assigned to the transitions: ^{2}B$_1$g→^{2}A$_1$g (dx^2–y^2→dz^2) (ν_1), ^{2}B$_1$g→^{2}B$_2$g (dx^2–y^2→dzy) (ν_2), respectively and third band may be due to charge transfer. The complex may have square–planar geometry[25].

3.4. Ligand field parameters

Various ligand parameters were calculated for the complexes and are listed in Table 2. The value Dq in Co(II) complexes was calculated from transition energy ratio diagram using the ν_3/ν_2 ratio The Nephelauxetic parameter β was calculated by using the relation β = B(complex)/B(free ion), where B free ion for Mn(II), Fe(III), Co(II) is 928, 966, and 912 cm^{-1}. The β value lies in the range 0.33–0.97. These values indicate that the appreciable covalent character of metal ligand σ bond [24–27].

Table 2: Ligand field parameters of the complexes

Complex	Dq (cm^{-1})	B(cm^{-1})	β	LFSE (kJmol^{-1})	F_2	F_4	C	ν_2/ν_1
[Fe(DPTMEBPP)(NO$_3$)$_3$(H$_2$O)$_2$].6.75H$_2$O	1689	923	0.83	214	–	–	–	1.22
[Mn(DPTMEBPP)(OAc)$_2$(H$_2$O)$_2$].2H$_2$O	868	964	0.88	–	1234	87	3156	1.49
[Co(DPTMEBPP)(OAc)$_2$(H$_2$O)$_2$].2H$_2$O	1182	903	0.32	96	–	–	–	1.64
[Ni(DPTMEBPP)(OAc)$_2$(H$_2$O)$_2$].2H$_2$O	798	–	0.96	113	–	–	–	1.82

3.5. EPR Spectra

The EPR spectra of the Cu(II) complex was recorded as polycrystalline sample as well as solution at room temperature at different frequency. In the EPR spectrum of the Cu(II) complex (Figure 3) no band corresponding to ms = ±2 transition [22,24, 28– 33] was observed in the spectrum, ruling out any Cu–Cu interaction. The g tensor

values of Cu(II) complex can be used to derive the ground state. In octahedral geometry the unpaired electron lies in the dx^2-y^2 orbital giving ^2B_1g as the ground state with $g_\parallel > g_\perp$. The $g_\parallel$ and $g_\perp$ values were computed from the spectrum using DPPH free radicals as „g" marker. The $g_\parallel$ values are < 2.5 which shoes covalent character of the metal ligand bond.

The trend $g_\parallel > g_\perp > 2.0023$ observed for these complexes indicates that the unpaired electron is localized in dx^2-y^2 orbital of the Cu(II) ions and the spectral features are characteristics of axial symmetry [34,35].
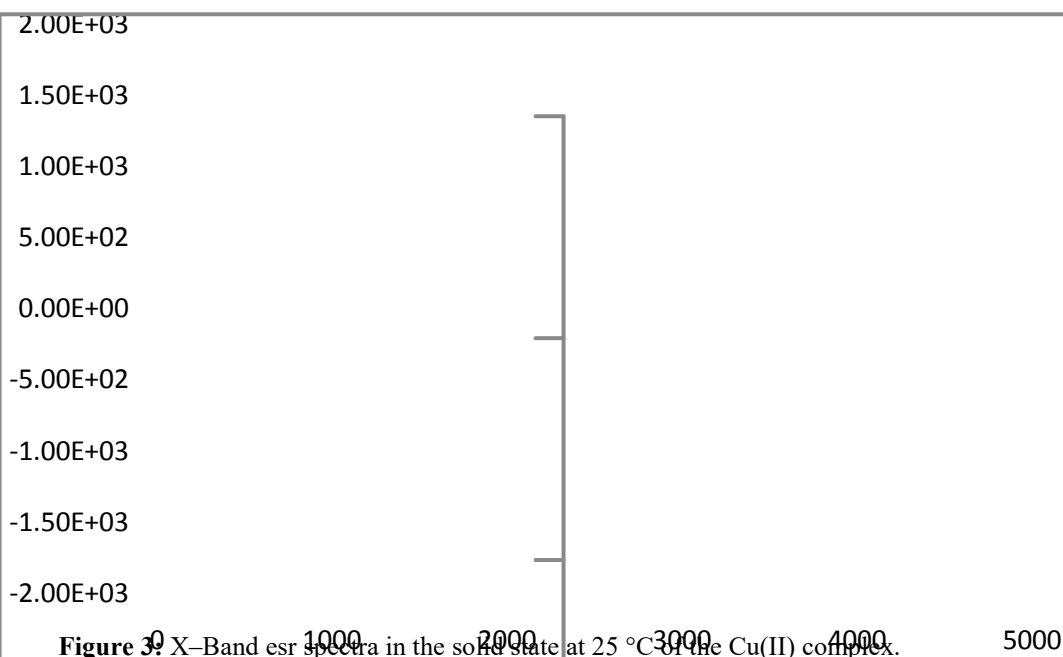
Figure 3: X–Band esr spectra in the solid state at 25 °C of the Cu(II) complex.

3.6. X–ray powder diffraction

Single crystals of the complexes could not be prepared to get the XRD and hence the powder diffraction data were obtained for structural characterization. Structures determination by X–ray powder diffraction (Fig. 4) data have gone through a recent surge since it have becomes important to get to the structural information of materials, which do not yield good quality single crystals. The

indexing procedures were performed using (CCP4, UK) CRYSFIRE program [36] giving cubic crystal system for [Co(DPTMEBPP)(OAc)$_2$(H$_2$O)$_2$].2H$_2$O (Fig. 4a) having M(6) = 14, F(6) = 8 and tetragonal crystal system for [Cu(DPTMEBPP)(OAc)$_2$].H$_2$O (Fig. 4b) having M(9) = 12, F(6) = 7 as the best solutions. Their cell parameters are shown in Table 3.
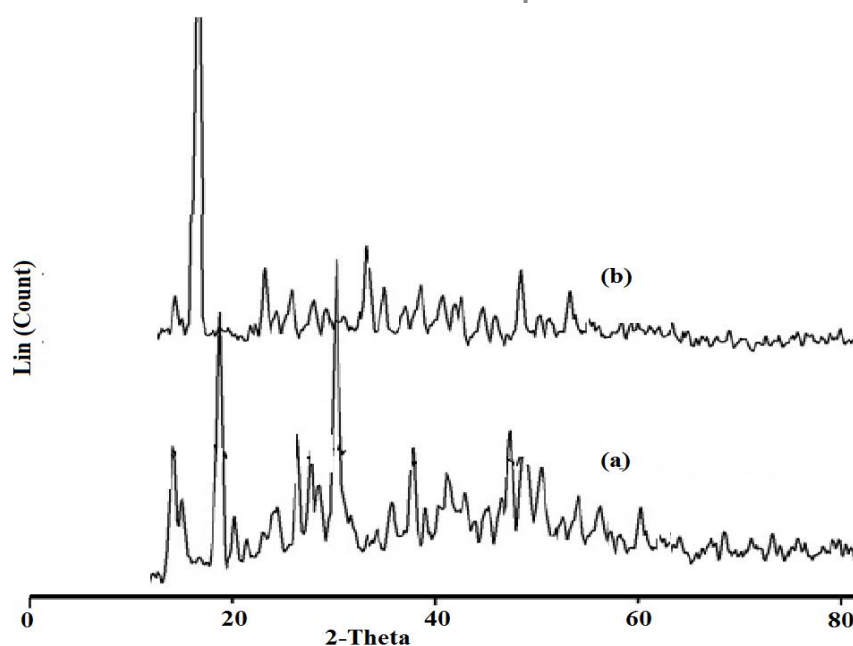
Figure 4: X–ray diffraction patterns of (a) Co(II) and (b) Co(II) complexes.

Table 3: Crystallographic data for the Schiff base complexes [Co(DPTMEBPP)(OAc)$_2$(H$_2$O)$_2$].2H$_2$O and [Cu(DPTMEBPP)(OAc)$_2$].H$_2$O.

Data	[Co(DPTMEBPP)(OAc)$_2$(H$_2$O)$_2$].2H$_2$O	[Cu(DPTMEBPP)(OAc)$_2$].H$_2$O
Empirical formula	[Co(DPTMEBPP)(OAc)$_2$(H$_2$O)$_2$].2H$_2$O	[Cu(DPTMEBPP)(OAc)$_2$].H$_2$O
Formula weight (g/mol)	771.57	722.14
Wavelength(Å)	1.54	1.54
Crystal system	Tetragonal	Cubic
Space group	P4/m	P4/m
Unit cell dimensions(Å)		
a(Å)	7.0112	15.147
b(Å)	7.0112	15.147
c(°)	15.8718	15.147
α(°)	90	90
β(°)	90	90
γ(°)	90	90
Volume (Å^3)	1103	6018
(Calc.) densit (g/cm^{-3})	1.83	1.21
2θ range	15.22–55.08	16.45–60..14
Limiting indices	0≤h≤3, 0≤k≤1, 1≤l≤7	3≤h≤10, 1≤k≤6, 3≤l≤10
Z	2	6
Rf	0.0000788	0.000019
Temperature (K)	298	298

3.7. Mass Spectra

The mass spectrum of the ligand (DPTMEBPP) showed a molecular ion peak at m/z 522.49. Fig. 2, which is equivalent to its molecular weight[37,38]. In addition to this, fragmented peak observed at m/z 88 is due to the cleavage of –(CHOCH$_3$)$_2$ group. The ESI-MS results of [Mn(DPTMEBPP)(OAc)$_2$(H$_2$O)$_2$].2H$_2$O, [Fe(DPTMEBPP)(NO$_3$)$_3$(H$_2$O)$_2$].6.75H$_2$O, [Co(DPTMEBPP)(OAc)$_2$(H$_2$O)$_2$].2H$_2$O, [Ni(DPTMEBPP)(OAc)$_2$(H$_2$O)$_2$].2H$_2$O, [Cu(DPTMEBPP)(OAc)$_2$].H$_2$O, [Zn(DPTMEBPP)(OAc)$_2$].2H$_2$O, [Pb(DPTMEBPP)-(OAc)$_2$].3H$_2$O and [La(DPTMEBPP)(Cl)$_3$(H$_2$O)$_2$].6H$_2$O showed [M]$^+$ peak at m/z 767.58, 903.97, 771.57, 771.33, 722.14, 741.99, 901.82 *and* 893.86 equivalent to their molecular weight respectively. All complexes and DPTMEBPP give the fragmentation of the 1,2,3–trimethoxy–5–methylbenzene group, which is observed at 79.2 m/z.

3.10. Thermal Analyses

TG for the complexes were carried out within a temperature range from room temperature up to 800 °C. TGA results are in a good agreement with the suggested formulae resulted from microanalyses data (Table 1).

The TGA data of Fe-complex of DPTMEBPP is thermally decomposed in three stages. The first stage corresponds to the loss of 4.164% of the weight of complex within the range 28.25-179.62°C corresponding to the loss of two water molecule of crystallization. The second stage corresponds to the loss of 11.531% of the weight of complex within the range 180.55-315°C corresponding to the loss of 3.25 water molecule of crystallization, one amino group and one methoxy group [CH$_3$O]$^+$. The last stage corresponds to the loss of 40.651% of the weight of the complex within the range 316-452°C that can be attributed to the loss of [C$_{19}$H$_{20}$N$_3$O$_3$P]$^+$. The residue 41.813% of the original weight of the complex, corresponds to the molecular weight of 378 mass unit which can be assigned for [C$_8$H$_{11}$FeN$_4$O]$^+$.

The TGA data of Cu–complex of DPTMEBPP is thermally decomposed in two stages. The first stage corresponds to the loss of 61.213% of the weight of complex within the range 21-341°C corresponding to the loss of one water molecule of crystallization and two acetate group associated with the complex and [C$_{14}$H$_{17}$N$_4$O$_4$]$^+$. The second stage corresponds to the loss of 18% of the weight of complex within the range 342-999°C corresponding to the loss of [C$_6$H$_7$OP]$^+$. The residue 20.765% of the original weight of the complex, corresponds to the molecular weight of 149.7 mass unit which can be assigned for CuO and [C$_6$H$_5$]$^+$.

The TGA data of Pb–complex of DPTMEBPP is thermally decomposed in five stages. The first stage corresponds to the loss of 5.845% of the weight of complex within the range 21–179°C corresponding to the loss of two water molecule of crystallization and one amino group. The second stage corresponds to the loss of 11.47% of the weight of complex within the range 180-373°C corresponding to the loss of 0.5 water molecule of crystallization and three methoxy group [CH$_3$O]$^+$. The third stage corresponds to the loss of 7.399% of the weight of the complex within the range 374–438°C that can be attributed to the loss of one acetate group associated with the complex. The fourth stage corresponds to the loss of 18.616% of the weight of the complex within the range 439-689°C that can be attributed to the loss of [C$_7$H$_6$O$_3$P]$^+$. The last stage corresponds to the loss of 5.78% of the weight of complex within the range 690–997°C that can be attributed to the loss of [C$_4$H$_5$]$^+$. The residue 50.632% of the original weight of the complex, corresponds to the molecular weight of 456.7 mass unit which can be assigned for [C$_{17}$H$_{16}$N$_2$Pb]$^+$.

The TGA data of La-complex of DPTMEBPP is thermally decomposed in two stages. The first stage corresponds to the loss of 49.635% of the weight of complex within the range 27–534°C corresponding to the loss of four water molecule of crystallization and [C$_{14}$H$_{17}$N$_4$O$_6$P]$^+$. The second stage

corresponds to the loss of 22.407% of the weight of complex within the range 536-998°C corresponding to the loss of $[C_{12}H_{10}O_3]^+$. The residue 27.88% of the original weight of the complex, corresponds to the molecular weight of 242 mass unit which can be assigned for $LaCl_3$.

3.11 Kinetic Studies

The thermodynamic activation parameters (Table 4–6) of decomposition processes of the metal complexes namely activation energy (E^*), entropy (ΔS^*) and Gibbs free energy change of the decomposition (ΔG^*) were evaluated graphically by employing three methods, Horowitz–Metzger [39] (HM), Coats–Redfern [40] (CR), and Piloyan–Novikova [41] (PN). From the results obtained, the following remarks can be pointed out:

1) The energy of activation (E) values increases on going from one decomposition stage to another for a given complex, indicating that the rate of decomposition decreases in the same order. Generally stepwise stability constants decreases with an increase in the number of ligand attached to a metal ion. Conversely, during decomposition reaction the rate of removal of remaining ligands will be smaller after the expulsion of the ligand [42,43].

2) The values of ΔG increases significantly for the subsequently decomposition stages due to increasing the values of (TΔS) from one stage to another. This may be attributed to the structural rigidity of the remaining complex after the expulsion of more ligands, as compared with the precedent complex, which require more energy, TΔS, for its rearrangement before undergoing any compositional change [44, 45].

3) The negative ΔS values for the decomposition steps indicate that all studied complexes are more ordered in their activated states [44].

4) The positive ΔH values mean that the decomposition processes are endothermic [46].

Table 4: Kinetic parameters evaluated by Coats–Redfern equation

Complex	Stage	T(K)	A(S⁻¹)	E_a (kJ/mol)	ΔH (kJ/mol)	ΔS (kJ/mol K)	ΔG (kJ/mol)
[Fe(DPTMEBPP)(NO₃)₃(H₂O)₂].6.75H₂O	1st	436	21.03 ×10⁵	169.88	112.22	−0.045	163
	2nd	567	48.77× 10⁷	188.39	125.69	−0.065	196
	3rd	798	73.39× 10¹⁰	197.33	154.48	−0.075	232
[Cu(DPTMEBPP)(OAc)₂].H₂O	1st	432	48.87 ×10⁶	68.56	68.75	−0.085	159
	2nd	587	22.64× 10⁷	134.88	98.38	−0.110	188
	3rd	800	58.75× 10⁹	176.53	123.89	−0.166	225
[Pb(DPTMEBPP)-(OAc)₂].3H₂O	1st	457	95.49 ×10⁷	134.73	97.12	−0.036	158
	2nd	507	24.89× 10⁷	158.82	134.88	−0.066	182
	3rd	794	97.32× 10⁹	188.63	154.43	−0.077	249
[La(DPTMEBPP)(Cl)₃(H₂O)₂].6H₂O	1st	448	12.77×10⁹	58.58	64.74	−0.029	166
	2nd	569	8.65×10¹¹	85.78	64.38	−0.077	183
	3rd	800	16.94×10⁶	133.84	94.64	−0.085	198

Table 5: Kinetic parameters evaluated by Horowitz–Metzger equation

Complex	Stage	T(K)	A(S⁻¹)	E_a (kJ/mol)	ΔH (kJ/mol)	ΔS (kJ/mol K)	ΔG (kJ/mol)
[Fe(DPTMEBPP)(NO₃)₃(H₂O)₂].6.75H₂O	1st	436	21.78 ×10⁵	169.74	112.43	−0.045	162
	2nd	567	48.94× 10⁷	188.12	125.71	−0.065	194
	3rd	798	73.32× 10¹⁰	197.36	154.49	−0.075	231
[Cu(DPTMEBPP)(OAc)₂].H₂O	1st	432	48.98 ×10⁶	68.42	68.74	−0.085	160
	2nd	587	22.70× 10⁷	134.75	98.59	−0.110	189
	3rd	800	58.87× 10⁹	176.53	124.71	−0.166	224
[Pb(DPTMEBPP)-(OAc)₂].3H₂O	1st	457	95.58 ×10⁷	134.76	96.96	−0.036	158
	2nd	507	24.76× 10⁷	158.97	134.69	−0.066	181
	3rd	794	97.22 × 10⁹	188.96	154.46	−0.077	250
[La(DPTMEBPP)(Cl)₃(H₂O)₂].6H₂O	1st	448	12.61×10⁹	58.97	64.38	−0.029	167
	2nd	569	8.34×10¹¹	85.95	64.55	−0.077	182
	3rd	800	16.74×10⁶	133.94	94.05	−0.085	199

Table 6: Kinetic parameters evaluated by Piloyan–Novikova equation

Complex	Stage	T(K)	$A(S^{-1})$	E_a (kJ/mol)	ΔH (kJ/mol)	ΔS (kJ/mol K)	ΔG (kJ/mol)
[Fe(DPTMEBPP)(NO$_3$)$_3$(H$_2$O)$_2$].6.75H$_2$O	1st	436	21.69×10^5	169.86	112.34	−0.046	164
	2nd	567	48.85×10^7	188.34	125.68	−0.064	196
	3rd	798	73.21×10^{10}	197.38	154.43	−0.076	233
[Cu(DPTMEBPP)(OAc)$_2$].H$_2$O	1st	432	48.86×10^6	68.58	68.96	−0.086	159
	2nd	587	22.53×10^7	134.83	98.41	−0.111	187
	3rd	800	58.34×10^9	176.59	123.96	−0.167	224
[Pb(DPTMEBPP)-(OAc)$_2$].3H$_2$O	1st	457	95.73×10^7	134.77	97.03	−0.035	159
	2nd	507	24.88×10^7	158.89	134.97	−0.065	183
	3rd	794	97.89×10^9	188.75	154.47	−0.076	249
[La(DPTMEBPP)(Cl)$_3$(H$_2$O)$_2$].6H$_2$O	1st	448	12.73×10^9	58.66	64.99	−0.024	166
	2nd	569	8.53×10^{11}	85.73	64.46	−0.074	184
	3rd	800	16.88×10^6	133.90	94.41	−0.088	197

3.15 Conclusions

The synthesized diphenyl (2-amino-5-(3,4,5-trimethoxybenzyl)pyrimidin-4-yl-phosphoramide (DPTMEBPP) act as bidentate ligand. The metals are coordinated to azomethine nitrogen and phenolic oxygen atoms. The analytical, IR, NMR, ESR, XRD, mass, electronic, magnetic, and thermal studies confirm the bonding of phosphoramidate ligand (DPTMEBPP) to metal ions. All these observations put together lead us to propose the following structure (Fig. 5) in which, the complexes having the stoichiometry of the type [M(III)L(H$_2$O)$_n$Yx].zH$_2$O (M = Fe(III); n= 2, Y=NO$_3$, x=3, Z= 6.75H$_2$O and M=La(III); n= 2, Y=Cl, x=3, Z= 6H$_2$O) and [M(II)L (OAc)$_2$(H$_2$O)$_n$].XH$_2$O (M = Mn(II); n= 2, X=2, M = Co(II); n= 2, X=2, M = Ni(II); n= 2, X=2, M = Cu(II); n= 0, X=1, M = Zn(II); n= 0, X=2 and M = Pb(II); n= 0, X=3)[L = DPTMEBPP].
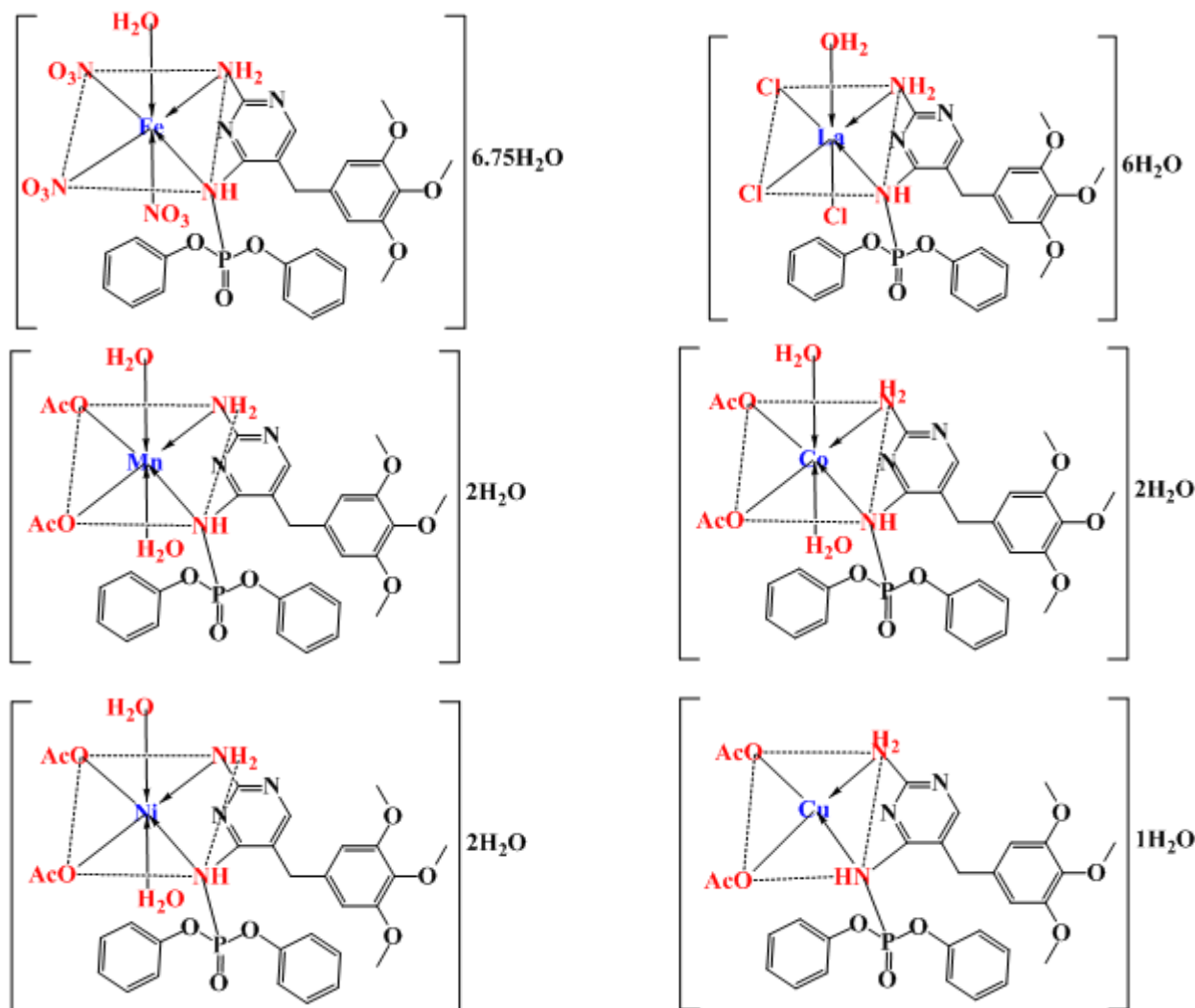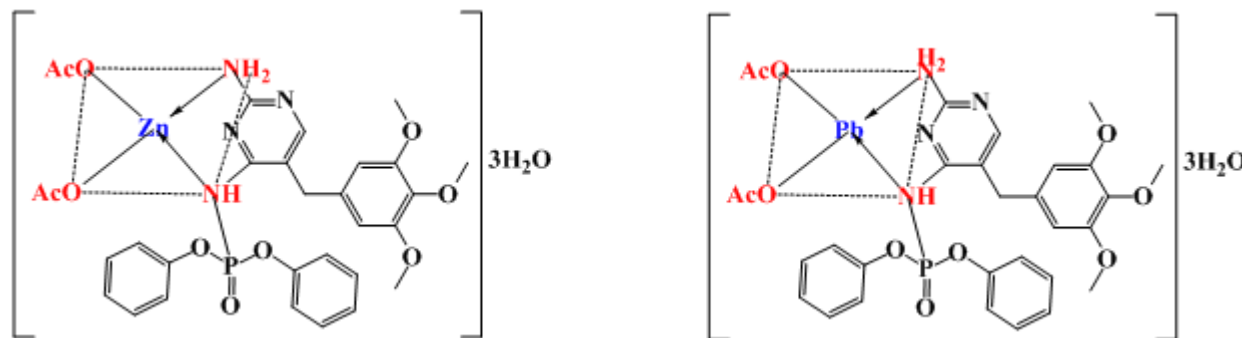
Figure 4: Proposed structures of the metal complexes

References

[1] N. Demirezen, D. Tarınç, D. Polat, M. Çeşme, A. Gölcü, M. Tümer, Spectrochimica Acta A 94 (2012) 243– 255.

[2] P.J. Sadler, Adv. Inorg. Chem. 36 (1991) 1–48.

[3] N. Saha, S. Kar, J. Inorg. Nucl. Chem. 39 (1977) 195–200.

[4] D. Kovala, N. Hadjiliadis, J. Tsangaris, J. Less Common Met. 115 (1986) 1–5.

[5] J. Tsangaris, D. Sotiropoulos, A. Galinos, Inorg. Nucl. Chem. Lett. 14 (1978) 445–449.

[6] F. Demartin, M. Manassero, L. Naldini, M. Zoroddu, Inorg. Chim. Acta 213 (1983) L213–L214.

[7] L. Naldini, M. Cabras, M. Zoroddu, F. Demartin, M. Manassero, M. Sansoni, Inorg. Chim. Acta 88 (1984) 45–50.

[8] M. Zoroddu, L. Naldini, F. Demartin, N. Masciocchi, Inorg. Chim. Acta 128 (1987) 179–183.

[9] F. Demartin, N. Masciocchi, L. Naldini, A. Panzanelli, M. Zoroddu, Inorg. Chim. Acta 171 (1990) 229–233.

[10] P.T. Muthiah, J.J. Robert, J. Chem. Crystallogr. 29 (1999) 223–226.

[11] B. Seekhon, H. Randhawa, H. Sahai, Synth. React. Inorg. Met.-Org. Chem. 29 (1999) 309–321.

[12] J.E. Weder, C.T. Dillon, T.W. Hambley, B.J. Kennedy, P.A. Lay, J.R. Biffin, H.L. Regtop, N.M. Davis, Coord. Chem. Rev. 232 (2002) 95–126.

[13] P.A. Ajibade, G.A. Kolawole, Transit. Met. Chem. 33 (2008) 493–497.

[14] M.J. Clarke, Coord. Chem. Rev. 236 (2003) 207–231.

[15] P.A. Ajibade, G.A. Kolawole, Synth. React. Inorg. Met.-Org. Chem. 40 (2010) 273–278.

[16] N. Demirezen, D. Tarınç , D. Polat, M. Çeşme, A. Gölcü, M. Tümer, Spectrochimica Acta A 94 (2012) 243– 255.

[17] L. Rajith, K.G. Kumar, Drug Test. Anal. 2 (2010) 436–441.

[18] A.M.A. Alaghaz, R.A. Ammar, European Journal of Medicinal Chemistry 45 (2010) 1314-1322.

[19] A.M.A. Alaghaz, Journal of Molecular Structure 1068 (2014) 27-4245.

[20] A.M.A. Alaghaz, A.G. Al-Sehemi, T.M. EL-Gogary, Spectrochimica Acta Part A: Molecular and Biomolecular Spectroscopy *95* (*2012*) *414-422*.

[21] A.M.A. Alaghaz, R.A.A. Ammar, G.Koehler, K.P. Wolschann, T.M. El-Gogary, Spectrochimica Acta Part A: Molecular and Biomolecular Spectroscopy *128* (*2014*) 724-729.

[22] K. Nakamoto, Infrared Spectra of Inorganic and Coordination Compounds, Wiley Interscience, New York, 1970.

[23] A.B.P. Lever, Crystal Field Spectra. Inorganic Electronic Spectroscopy, first ed., Elsevier Amsterdam, 1968.;A.B.P. Lever, Electronic Spectra of Inorganic and Coordination Compounds, John Wiley, New York, 1968.

[24] A. M.A. Alaghaz, Molec. Struct. 1072 (2014) 103–113.

[25] A.B.P. Lever, Inorg. Electronic Spectroscopy, second ed. Elsevier, Amsterdam, 1984.

[26] A. M.A. Alaghaz, B. A. El-Sayed, A. A. El-Henawy, R. A.A. Ammar, Molecu. Struct. 1035 (2013) 83–93.

[27] R.S. Drago, Physical Methods in Chemistry, W.B. Saunders Company, London, 1977.

[28] D.M. Hong, H.H.Wei, L.L. Gan, G.H. Lee,Y.Wang, Polyhedron 15 (1996) 2335.

[29] S. Chandra, S.D. Sharma, Trans. Met. Chem. 27 (2002) 733.

[30] A. Abragam, B. Bleaney, Electron Paramagnetic Resonance of Transition Ions, Oxford University Press, Oxford, 1970.

[31] F.E. Mabbs, D. Collison, Electron Paramagnetic Resonance of Transition Metal Compounds, Elsevier, Amsterdam, 1992.

[32] S. Chandra, R. Kumar, Spectrochimica Acta Part A 66 (2007) 74–80.

[33] J. Owen, Proc. Roy. Soc. London, A 227 (1955) 183.

[34] S.V. Rosoka, Y.D. Lampeka, I.M. Maloshtan, Dalton Trans. (1993) 631.

[35] S. Chandra, Ruchi, Spectrochimica Acta Part A 103 (2013) 338–348.

[36] B. Singh, B.P. Yadav, R.C. Aggarwal, Ind. J. Chem A. 23 (1984) 441–444.

[37] S. Chandra, R. Gupta, N. Gupta, S.S. Bava, Synth. React. Inorg. Metal–Org. Nano–Met. Chem. 35 (2005) 883–888.

[38] R. Shirley, The CRYSFIRE System for Automatic Powder Indexing: User's Manual, Lattice Press, 2002.

[39] H.H. Horowitz, G. Metzger, Anal. Chem. 35 (1963) 1464–1468.

[40] A.W. Coats, J.P. Redfern, Nature 20 (1964) 68–69.

[41] G.O. Piloyan, T.D. Pyabonikar, C.S. Novikova, Nature, 212 (1966) 1229–1304.

[42] T. Taakeyama, F.X. Quinn, Thermal Analysis Fundamentals and Applications to Polymer Science, John Wiley and Sons, Chichester, 1994.

[43] P.B. Maravalli, T.R. Goudar, Thermochim. Acta 325 (1999) 35–41.

[44] K.K.M. Yusuff, R. Sreekala, Thermochim. Acta 159 (1990) 357–368.

[45] S.S. Kandil, G.B. El–Hefnawy, E.A. Baker, Thermochim. Acta 414 (2004) 105–113.

[46] L.T. Valaev, G.G. Gospodinov, Thermochim. Acta 370 (2001) 15–19.

Paper ID: NOV152999

1229